Numerical study of natural convection in partially open tilted cavities with different boundary surfaces conditions

Ahmed M. Abdel-Latif [a] and Taib El-Bakoush [b]
[a] *Mechanical Power Eng. Dept., Faculty of Eng., Zagazig University, Zagazig, Egypt*
[b] *Mechanical Eng. Dept., Faculty of Eng., Al-Margheb University, El-Khomss, Libya*

A numerical study of two-dimensional laminar natural convection has been carried out on partially open tilted cavities with different wall boundary conditions. Four different boundary conditions were studied: (a) case (A), the wall inside the cavity facing the opening and the lower wall are isothermal and the remaining walls are adiabatic, (b) case (B), the wall inside the cavity facing the opening and the upper wall are isothermal and the remaining walls are adiabatic, (c) case (C), the upper and lower walls are isothermal and the remaining walls are adiabatic, (d) case (D), the wall inside the cavity facing the opening, the lower and the upper walls are isothermal and the remaining walls are adiabatic. Dimensionless aperture size ranging from 0.25 to 0.75, with different positions (different values of d/H): high, center and low is studied. Steady-state solutions are presented for Rayleigh number between 10^3 to 10^5 and for tilt angles ranging from 0^o (the opening facing upward) to 120^o. The fluid considered is air with Prandtl number fixed at 0.704. Equations of continuity, momentum and energy are solved using constant properties and Boussinesq approximation. It is found that tilt angle, wall boundary conditions, aperture size and position are all factors that strongly affect the convective heat transfer coefficient between the cavity and the ambient air. At low Ra, wall boundary conditions have a minimal effect on $\overline{Nu}$. However, increasing Ra, the wall boundary conditions have greater effect on the Nusselt number. The average Nusselt number ($\overline{Nu}$) is generally lower at low inclination angles ($\alpha \leq 30^o$), and attains its highest value when the cavity is horizontal ($\alpha = 90^o$). Depending on the application, which may require maximizing or minimizing of heat transfer through the aperture, the wall boundary conditions, aperture size, its position and inclination angle should be chosen as design parameters.

ناقش هذا البحث عملية أنتقال الحرارة بالحمل الحر داخل تجويف مائل ومفتوح جزئيا مع ظروف جدارية مختلفة. وقد تمت الدراسة لأربعأنواع مختلفة من الظروف الجدارية وهى كالآتى: (أ) النوع الأول وفيه الجدار الداخلى للتجويف والمقابل للفتحة الجزيئية وكذلك لجدار السفلى ذوى درجات حرارة ثابته التجويف معزولة. (ب) النوع الثانى فيه الجدار الداخلى للتجويف والمقابل للفتحة الجزيئية وكذلك العلوى ذوى درجات حرارة ثابته وباقى سجدران التجويف معزولة. (ج) النوع الثالث وفيه الجداران العلوى الصفلى ذوى درجات حرارة ثابته وباقى جدران التجويف معزولة. (د) النوع الرابع وفيه الجدار الداخلى للتجويف والمقابل للفتحة الجزيئية وكذلك الجداران العلوى والسفلى ذو درجات حرارة ثابتة والجدران الباقية للتجويف معزولة. وقد تم الأخذ فى الأعتبار أهم المؤثرات وتشمل الآتى: حجم الفتحة الجزيئية والتى كانت تتغير من ٠,٢٥ الى ٠,٧٥، موضع هذه الفتحة (علوية – سفلية – مركزية)، زاوية ميل التجويف وكانت تتغير من صفر الى ١٢٠ درجة، عدد رايلى وتم تغيير من ١٠ ^{٣} الى ١٠ ^{٥}. ولق تم حل معادلات الكتلة والحركة والطاقة مع ثبات الخواص لحالة الحمل الحر الأنسيابى. ووجد أن الحدود الجدراية وزاوية ميل التجويف وحجم الفتحة الجزيئية ومكانها كلها من العوامل التى تؤثر بشدة على معامل انتقال الحرارة من التجويف الى الهواء الخارجى. أيضا وجد أن تأثير الحدود الجداريه على عملية أنتقال الحرارة عند عدد رايلى المرتفع يكون أشد منه فى الحالات التى لها عدد رايلى منخفض. كذلك بينت الدراسة أن معدلات انتقال الحرارة للنوع الرابع من الحدود الجدارية أعلى من الأنواع الأخرى التى تم دراستها. وختمت الدراسة ببيان لأهم النتائج التى تم التوصل اليها والتوصيات المقترحة.

Keywords: Natural convection, Partially open cavity, Wall boundary conditions, Inclined cavity

1. Introduction

Natural convection from partially open cavities has many significant engineering applications, including electronic cooling devices, open cavity solar thermal receivers, uncovered flat solar collectors having rows of vertical strips, thermal design of buildings, and aircraft break-housing systems design. In all these applications there is a cavity with one or more of its sides heated or at adiabatic conditions. For example, in electronic equipment

the electronic boards can present a heat source that affects the temperature of the board while the rest of the walls of the enclosing box can be considered as insolated walls. A literature review shows that numerous studies have been published on a square open cavity. Excluding a series of experimental studies at a specific Rayleigh number, most of these studies have been carried out with fully open horizontal cavities having isothermal walls or the wall facing the opening is isothermal and others are adiabatic.

Various authors studied experimentally open cavities [1-6]. Sernas and Kyriakides [1] experimentally studied two-dimensional, laminar natural convection in an open cavity filled with air as a working fluid with cavity aspect ratio of unity. The dimensionless aperture size in Hess and Henze [2] was 0.5 and it was centrally located in a square cavity. They used a laser Doppler velocimetry and flow visualization techniques to study flow characteristics and determined local Nusselt number at various levels covering Rayleigh number from 10^7 to 10^{11} in laminar and turbulent regimes. Chan and Tien [3] performed an experimental study for natural convection in a two-dimensional open rectangular cavity. Water was used as the working fluid in this experiment. It was observed at low Rayleigh numbers that the fluid exits the cavity as a buoyant "plume" while at higher Rayleigh numbers, the exit velocities are high enough to form a buoyant "jet". The effect of the open boundary was found to consist of two parts: the outgoing hot fluid exhibiting strong characteristics of the cavity conditions and incoming flow influenced by the outside conditions. Showole and Tarasuk [4] studied laminar natural convection heat transfer from isothermal open cavities experimentally using a Mach-Zehnder interferometer and numerically by a finite difference technique. Their work dealt with selected cavity aspect ratio of 0.25, 0.5 and 1, for Rayleigh numbers Ra ranging from 10^4 to 5×10^5, and for tilt angles α = 0.0°, 30°, 45°, and 60°. Flow and temperature patterns, velocity and temperature profiles, and local and average heat transfer rates were presented. Chakroun et al. [5] studied fully and partially open inclined cavities with aperture size from 0.25 to 1, aperture located centrally. Grashof number was 5.5×10^8 and constant. Later using the same experimental set-up, they studied the effect of aperture location in an inclined square cavity with isothermal heated walls at the same Grashof number [6].

Others studied theoretically natural convection heat transfer in fully open cavities [7-12]. Penot [7] conducted a numerical study of two-dimensional natural convection in an isothermal open square enclosure. The governing equations were solved in an enlarged computational domain by utilizing the far field boundary conditions. The effect of inclination and Grashof number were studied in this investigation. Chan and Tien [8] performed a numerical steady-state study of laminar natural convection in a two-dimensional square open cavity with a heated vertical wall and two insulated horizontal walls. Calculations were made in an extended computational domain beyond the aperture plane for cavity with a heated vertical wall and two horizontal insulated walls. Results obtained for Rayleigh number ranging from 10^3 to 10^9 were found to approach those of natural convection over a vertical isothermal flat plate. Elsayed et al. [9] studied numerically natural convection in fully open tilted cavities. Effects of the controlling parameters (Grashof number and tilt angle) on the heat transfer (average Nusselt number) were presented and analyzed. Chan and Tien [10,11] examined natural convection inside square and shallow open vertical cavities for different Rayleigh numbers. They made a comparison study using a square cavity in an enlarged computational domain. The comparison showed that the Nusselt numbers do not agree well at low Rayleigh numbers (Ra = 10^3), although the flow patterns look similar. This discrepancy is attributed to the boundary condition that prescribes no heat transfer across the opening portion of the cavity where the flow is incoming; this assumption neglects the conduction moving upstream out of the cavity, which is significant at low Rayleigh numbers. However, as Ra increases to 10^6, the heat transfer parameters (Nusselt numbers, isotherms, and flow patterns) are almost identical in the two methods. Polat and Bilgen [12] studied numerically inclined fully open shallow cavities in which the side facing the opening was heated by

constant heat flux, two adjoining walls were insulated and the opening was in contact with a reservoir at constant temperature and pressure. The computational domain was restricted to the cavity.

Laminar natural convection heat transfer in partially open cavities with a discrete flush mounted iso-flux heat source on one of its wall was investigated numerically by Jilani et al. [13]. They found that Rayleigh number considerably affects the flow and thermal fields within the open enclosure when compared with intensity of heat flux and size of the opening. Bilgen and Oztop [14] studied numerically natural convection heat transfer in partially open inclined square cavities. The surface of the wall inside the cavity facing the partial opening was isothermal. Streamlines and isotherms were produced, heat and mass transfer was calculated.

Literature review shows that in the experimental studies with partially open cavities, either Rayleigh number was kept constant [5,6], or it was very high [2]. In the numerical study of the same problem, one wall was heated [13,14]. In the present study, we will analyze and present results obtained from a numerical study of partially open tilted cavities with different wall boundary conditions using an enlarged computational domain. Four cases of boundary wall conditions of the cavity were studied. Effect of dimensionless aperture size ranging from 0.25 to 0.75, with different positions (different position ratio d/H) on heat transfer characteristics were investigated. Also, effect of Rayleigh numbers between 10^3 to 10^5 and tilt angles from 0° (facing upward) to 120° (facing 30° downward) on heat transfer rates were analyzed.

2. Problem description and mathematical model

2.1. Problem description

A schematic of the two dimensional system is shown in fig. 1. The energy from the isothermal walls is dissipated by convection through the opening. Four different wall boundary conditions are considered as in table 1. Three dimensionless aperture size 0.25, 0.5, and 0.75 and three aperture positions (d/H = 0.75, 0.50, and 0.25) are examined. Five inclination angles, 0, 30, 60, 90 and 120° are carried out.

2.2. Mathematical model

The continuity, momentum and energy equations for a two dimensional laminar flow of an incompressible Newtonian fluid are written. The following assumptions are made: there is no viscous dissipation, the gravity acts in the vertical direction, fluid properties are constant and fluid density variations are neglected except in the buoyancy term (the Boussinesq approximation) and radiation heat exchange is negligible. In dimensionless form, the non-dimensional governing equations are written as:

$$\frac{\partial U}{\partial X}+\frac{\partial V}{\partial Y}=0\,, \tag{1}$$

$$U\frac{\partial U}{\partial X}+V\frac{\partial U}{\partial Y}=-\frac{\partial P}{\partial X}+Ra\,Pr\,\theta\cos\alpha+Pr\,\nabla^2 U\,, \tag{2}$$

$$U\frac{\partial V}{\partial X}+V\frac{\partial V}{\partial Y}= -\frac{\partial P}{\partial Y}+Ra\,Pr\,\theta\,sin\alpha+Ra\,Pr\,\theta+Pr\,\nabla^2 V\,, \tag{3}$$

$$U\frac{\partial \theta}{\partial X}+V\frac{\partial \theta}{\partial Y}=\nabla^2\theta\,. \tag{4}$$

It is convenient to define the following dimensionless quantities:

$$X=\frac{x}{L}\qquad Y=\frac{y}{L}$$
$$U=\frac{uL}{\alpha}\qquad V=\frac{vL}{\alpha}\,, \tag{5}$$

$$\theta=\frac{T-T_\infty}{T_H-T_\infty}\qquad P=\frac{(p-p_\infty)L^2}{\rho\alpha^2}$$

$Gr = g\beta\Delta TL^3/(\nu^2)$ $Ra = g\beta\Delta TL^3/(\nu\alpha)$.

As will be explained later, the steady-state solutions are obtained from unsteady-state eqs. (1 to 4).

The local and average Nusselt numbers are calculated respectively as:

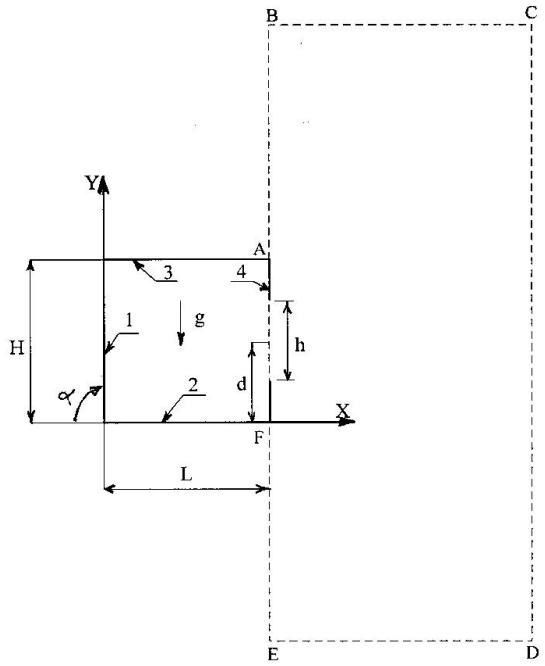

Fig. 1. Schematic of teh partially open cavity and coordinate systems.

$$Nu_{loc} = \frac{-\frac{\partial\theta}{\partial n}}{\theta}$$

$$\overline{Nu} = \sum_{1}^{j} \int_{0}^{A} Nu_{loc}\, d(XorY), \qquad (6)$$

where j is the number of heating surfaces, $d(X$ or $Y)$ denotes that, if the heating surface in X direction we take dX and if the heating surface in Y direction we take dY.

2.3. Boundary conditions

The boundary conditions of the system shown in fig. 1 are θ = 1 on the isothermal walls of the cavity, $\partial\theta/\partial n$ = 0 on the adiabatic boundaries of the cavity. θ = 0 on the free surface CD above the cavity. The walls AB and EF at the proximity of the aperture plane were taken to be adiabatic, i.e., $\partial\theta/\partial$X = 0. At the nonsolid boundaries BC and DE, the derivative boundary condition $\partial\theta/\partial$Y = 0 was used. At the solid boundaries, no slip and no penetration applied therefore, $U = V = 0$.

3. Numerical technique

The governing equations, given by eqs. (1 to 4) were discretized using a second order upwind interpolation scheme in FLUENT code [15]. The segregated solution algorithm is utilized to solve the system of equations. The advantage of using this method is that the global system matrix is decomposed into smaller sub-matrices and then solved in a sequential manner. This technique will result in considerably fewer storage requirements. The convergence criteria were specified as follows: the normalized residuals of all dependent variables must be less than 10^{-7}. To ensure the attainment of grid-independent results, the sensitivities of both grid numbers and grid distributions were tested for each case. Fig. 2 shows one of the results of the effect of grid size on the predicted U velocity at mid-plane distribution for the case of isothermal wall facing the central partial opening of dimensionless size h/H = 0.5 (α = 90°, Ra = 10^5). Typically, a grid density of 50×50 provides satisfactory solution for the case shown. Similar tests were done with the cavities having different boundary conditions, different aperture size and inclination, and the grid sizes were adjusted accordingly. The code was executed on 2.0 GHz clock speed, the execution time, at Ra = 10^5 for example, was 280 s.

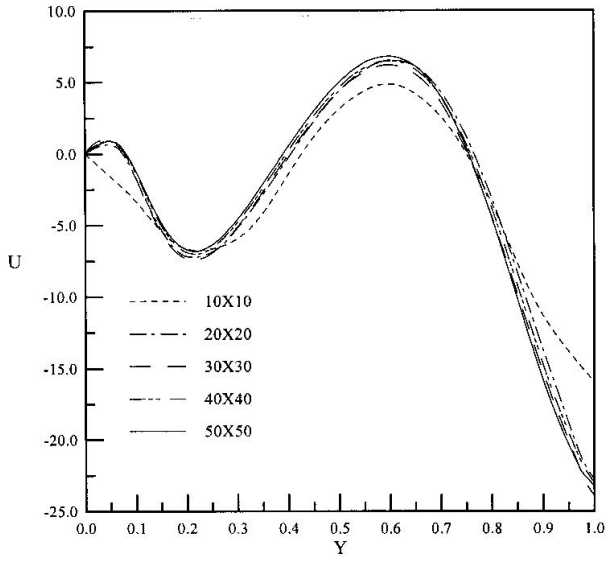

Fig. 2. Effect of grid size on the predicted U velocity at midplane (α = 90 °, h/H = 0.5, Ra = 10^5).

3.1. Validation

To validate the code, the case of a horizontal fully open square cavity having an isothermal wall reported by Chan and Tien [10] and Bilgen and Oztop [14] was studied. Chan and Tien [10] used an extended computation domain while Bilgen and Oztop [14] used a computation domain restricted to the cavity and we used an extended computation domain. The results of comparison are presented in table 2. We can see an agreement between the present work and that of Chan and Tien [10]. Also, it is seen the deviation of results of Bilgen and Oztop [14] from that of the present work and that of Chan and Tien [10]. This deviation vary from 22.4% at low Rayleigh number to 1.3% at high Rayleigh number. The reason for the large deviations at low Rayleigh number is explained by the fact that the heat transfer is dominated by conduction regime and since the temperature at opening is set at $\theta = 0$ by [14], the temperature gradient is higher, hence Nusselt number is higher than that with enlarged computation domain case (present work and Chan and Tien [10]). This effect disappears gradually at high Rayleigh numbers as the heat transfer becomes convection dominated.

4. Results and discussion

A numerical study has been carried out to study the effect of wall boundary conditions of the cavity as well as the tilt angle on heat transfer and flow field for partially open cavity. Different wall configurations (case A, B, C, and D), as shown in table 1, were examined. Geometrical and thermal parameters governing the heat transfer and flow field in inclined partially open cavities are aspect ratio $A = L/H$, aperture size AR = h/H, opening position $AP = d/H$, inclination angle α, and Ra, see fig. 1. The geometrical cases are: three aperture sizes of 0.25, 0.5 and 0.75 located at center, high and low positions, nine in all.

Heat transfer and fluid flow through the cavity are examined for a range of Rayleigh number from 10^3 to 10^6, the aspect ratio of $A = 1$, the aperture size $AR = h/H$ of 0.25, 0.5 and 0.75, the aperture position $AP = d/H$ at 0.125 (the lowest dimensionless position), 0.5 and 0.875 (the highest dimensionless position) and inclination α from 0^o (the aperture facing upward) to 120^o (the aperture facing 30^o downward). All result are with $Pr = 0.704$.

4.1. Temperature and flow fields

Isotherms and streamlines for wall boundary condition case (A) with $A = 1$, $AR = h/H = 0.5$, $AP = d/H = 0.5$, $\alpha = 90^o$ are presented in fig. 3 for Rayleigh number from 10^3 to 10^6. We observe in fig. 3-a that the heat transfer in the cavity is quasi-conductive at $Ra = 10^3$ and becomes dominated by convective regime as Ra increases to 10^6 in fig. 3-b to 3-d. At $Ra = 10^3$, the streamlines in the cavity show that for quasi-conductive regime the entrance and exit sections of the fluid at the opening are almost equal. At $Ra = 10^4$ in fig. 3-b, the heat transfer is by conduction as well as convection and the increased contribution of convection is clearly. As Ra increases to 10^5, fig. 3-c shows that a convection regime is established: the cold fluid entrained through the larger section of the opening moves across the cavity following the lower hot wall, rises along the vertical hot wall, moves across the upper part following the top bounding wall and discharges at the opening. A convection cell is formed at the lower right corner as the fluid accelerates across the lower hot wall and toward the vertical hot wall and the larger circulating convection cell is not symmetric. The isotherms show a boundary layer heat transfer on the lower and vertical hot walls. Fig. 3- d, at $Ra = 10^6$, shows a similar trend to

Table 1
Cases of wall boundary conditions

Case	wall 1	wall 2	wall 3	wall 4
A	T_H	T_H	a	a
B	T_H	a	T_H	a
C	a	T_H	T_H	a
D	T_H	T_H	T_H	a

Notes: T_H = isothermal, a = adiabatic

Table 2
Comparison of the results with a horizontal fully open square cavity

Ra	*Nu* [10]	*Nu*[14]	*Nu* (this study)
10^3	1.07	1.31	1.07
10^4	3.41	3.53	3.39
10^5	7.69	7.85	7.71
10^6	15.00	15.2	15.3

the case with $Ra = 10^5$ with enhanced convection and boundary layer flow and heat transfer at the hot walls. We see that as Ra increases, the flow becomes fully convection dominated and the discharging fluid from the upper part of the cavity occupies smaller and smaller section of the opening, being a jet like at high Rayleigh numbers.

The effect of aperture size $AR = h/H$ is presented in fig. 4, for wall boundary condition case (A), with the case $AP = 0.5$, $Ra = 10^5$, $\alpha = 90^o$ for $AR = h/H = 0.25$ (smaller opening) and 0.75 (larger opening). The case for AR = 0.5 is shown in fig. 3-c. It is seen that as expected the cold fluid's acceleration is higher for $AR = h/H = 0.25$ and smaller for $AR = h/H = 0.75$. We see that convection is enhanced with larger opening and the reverse is the case for smaller opening, this trend may be expected since the resistance to flow in and out the cavity will be smaller in the former case.

The effect of the position of the opening for wall boundaries case (A) is presented in fig. 5, with $AR = 0.5$, $Ra = 10^5$, $\alpha = 90^o$ with AP = $d/H = 0.75$ (high position) and 0.25 (low position). The case for $AP = 0.5$ is shown in fig. 3-c. These two correspond to upper and lower half openings respectively. It is seen that in fig. 5-a that the cold fluid enters the cavity at the lower part of the opening, accelerates to the vertical hot wall leaving right lower part of the cavity where a secondary convection cell is formed. The isotherms show that the right lower part of the cavity remains cold, where the main circulation is formed. Fig. 5-b shows the case with low aperture position ($AP = 0.25$) in which case the air enters the cavity similarly at the lower part of the opening and flows parallel to the lower hot wall and flows towards the vertical hot wall and exit at the upper part of the opening. The fluid sweeps the entire cavity except the right upper corner. The isotherms show that the upper right corner of the cavity remains cold. In comparing results in figs. 3-c, 5-a, and 5-b, it appears that all the parameters being the same, at the low aperture position the convection is highest, as a result of which heat transfer should be better. Between the center and high positions, the convection is stronger in center position aperture.

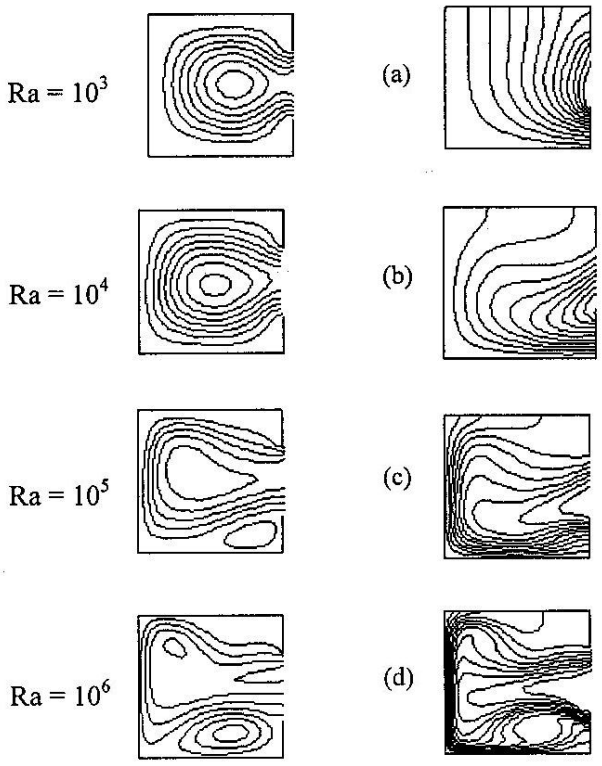

Fig. 3. Flow (on the left) and temperature (on the right) fields for boundary walls type (A), AR = h/H = 0.5, AP = 0.5, $\alpha = 90^o$ (a) (a) Ra = 10^3, (b) Ra = 10^4, (c) Ra = 10^5, and (d) Ra = 10^6.

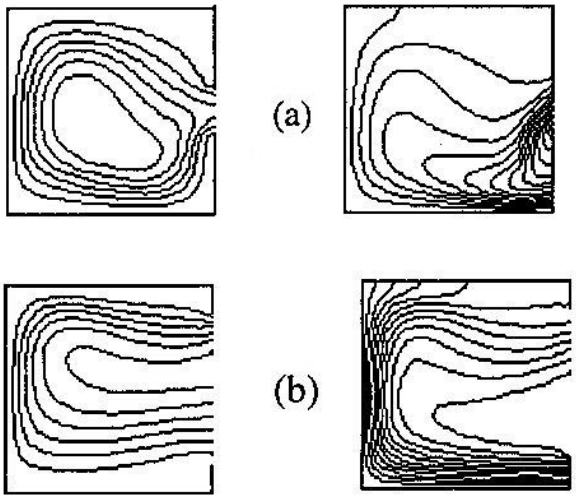

Fig. 4. Flow (on left) and temperature (on right) fields for boundary walls type (A) with the case AP = d/H = 0.5, $\alpha = 90^o$ and Ra = 10^5 (a) AR = h/H = 0.25, (b) AR = h/H = 0.75.

The effect of the wall boundary conditions is presented in fig. 6, for $AR = h/H = 0.5$, $\alpha = 90^o$, $AP = d/H = 0.25$ and $Ra = 10^5$ with wall boundary conditions cases (B), (C), and (D). The case (A) is shown in fig. 5-b. It is seen that the flow fields are similarly for all cases, in which air enters the cavity at the lower part of the opening and flows parallel to the lower wall and passes toward the vertical wall and exit at the upper part of the opening. The isotherms for wall boundary conditions case (A) and case (D) are similar, since the upper heated wall has a small effect on convection mechanism. In comparing results in fig. 6-a and 6-b, it appears that, at the boundary wall condition case (C), the convection is highest as a result of which heat transfer should be better.

The effect of inclination is presented in fig. 7 for wall boundary conditions case (A) with the case $AR = h/H = 0.5$, $AP = d/H = 0.5$, $Ra = 10^5$ for $\alpha = 30^o$, 60^o, and 120^o. The case for $\alpha = 90^o$, is shown in fig. 3-c. At $\alpha = 30^o$, the streamlines in fig. 7-a give an indication of flow separation at the lower edge of the opening and flow reattachments at the upper part of the wall facing the opening where a secondary convection cell is formed. The isotherms reveals that at the point of flow separation the temperature gradient is lower than at the reattachment point where the highest gradient are observed. The case with $\alpha = 60^o$ shown in fig. 7-b has the same appearance as that of fig. 7-a, except that a two nonsymmetrical cells are formed in the cavity one from separation and the other from reattachment. As α increases (greater than 60^o), the flow that separates at the lower edge of the opening reattaches on the base of the cavity and a single strong convection cell are formed in the cavity. At $\alpha = 90^o$, 120^o as shown in fig. 3-c and fig. 7-c respectively, the rate of inflow and outflow of air into and out of the cavity appear to be more rapid that at $\alpha = 30^o$. The isotherms reveals that the convection strengths at $\alpha > 60^o$ are greater than those at $\alpha \leq 60^o$.

4.2. Velocity and temperature profiles

Non-dimensional velocity and temperature profiles at mid-planes are presented in fig. 8

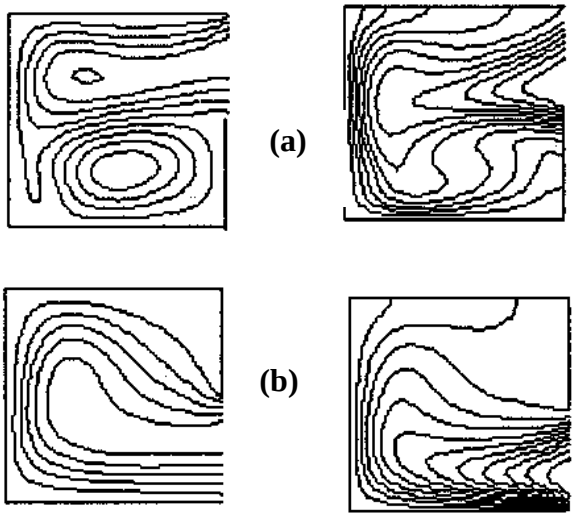

Fig. 5. Flow (on the left) and temperature (on the right) fields for boundary walls type (A) with the case $AP = d/H = 0.5$, $\alpha = 90^o$ and $Ra = 10^5$ (a) $AR = h/H = 0.75$, (b) $AR = h/H = 0.25$.

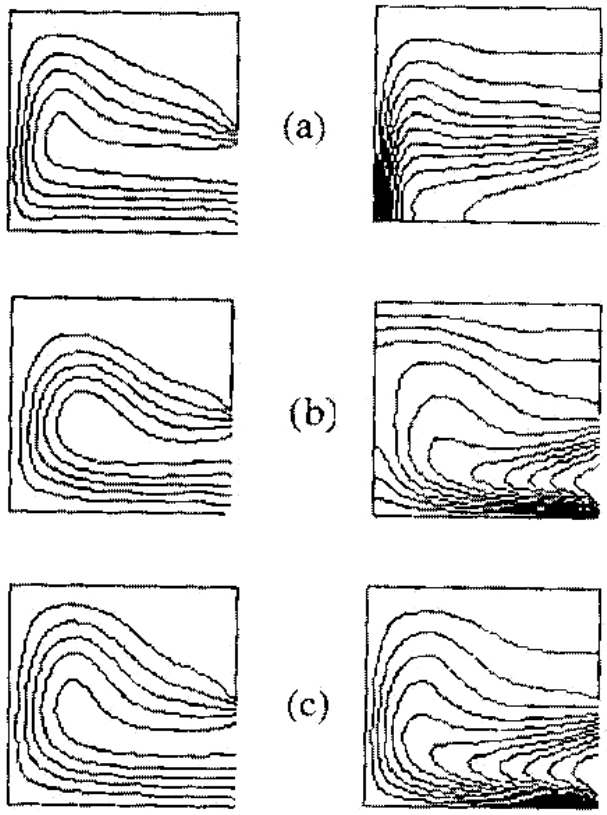

Fig. 6. Flow (on the left) and temperature (on the right) fields for the case $AR = h/H = 0.5$, $\alpha = 90^o$ and $AP = d/H = 0.25$ and $Ra = 10^5$ (a) boundary walls type (B), (b) boundary walls type (C), (c) boundary walls type (D).

for various boundary wall conditions with the case $AR = AP = 0.5$, $\alpha = 90^o$, $Ra = 10^5$. We can see that for the horizontal case with $\alpha = 90^o$, the velocity at the mid-plane is almost symmetric for all boundary wall condition types. The cold fluid enters the cavity at the lower part of the opening, where the velocities have a maximum negative values, and the hot fluid exit at the upper part of the opening, where the velocities have a positive values, as expected from earlier observations. Also, fig. 8-a shows that, the boundary wall conditions have an affect in increasing the flow strength. Fig. 8-b shows variation of temperatures at mid-plane for various boundary wall conditions, in this figure the curve of boundary condition case (A) concedes with that of case (B). It is clearly observed that the incoming ambient fluid ($\theta = 0$) is preheated before it reaches the back-wall boundary layer and the temperature increases with increasing Y for cases (A and B). However, as boundary wall condition changes, the preheating of the incoming fluid increases (as in cases (C) and (D)).

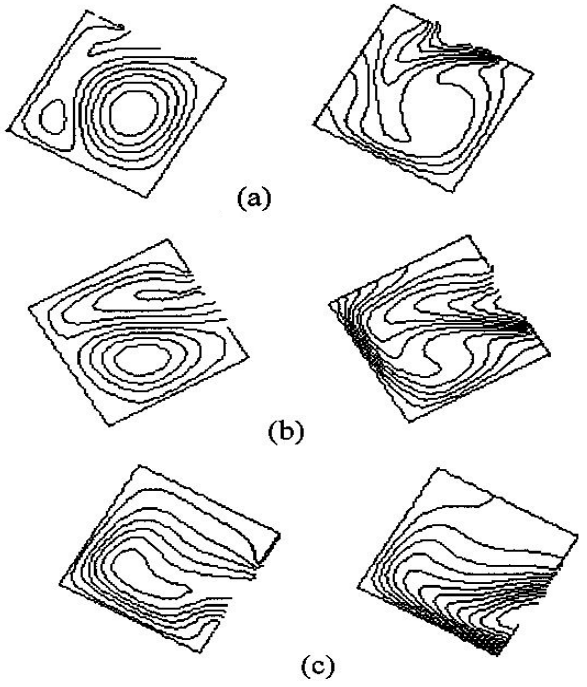

Fig. 7. Flow (on the left) and temperature (on the right) fields for the case boundary wall type (A) with the case $AR = h/H = 0.5$, $AP = d/H = 0.5$ and $Ra = 10^5$ for various inclination angle, (a) $\alpha = 30^o$ (b) $\alpha = 60^o$, (c) $\alpha = 120^o$.

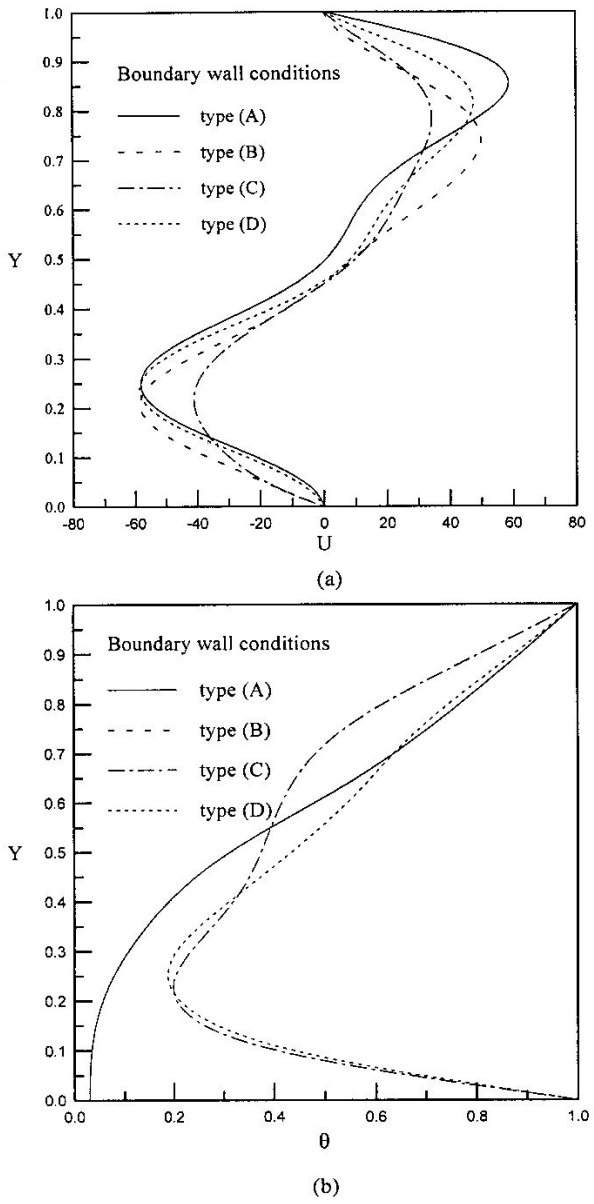

Fig. 8. Velocity and temperature profiles at mid-planes for various boundary wall condition with the case $AR = AP = 0.5$, $\alpha = 90^o$, $Ra = 10^5$.

4.3. Heat transfer rate

We will present first heat transfer, average Nusselt number $\overline{Nu}$ as a function of Rayleigh number *Ra*, *Ra* from 10^3 to 10^5 for different boundary wall conditions with the case of centrally located aperture of ($AP = AR = 0.5$) at inclination of 90^o. Then we will present the effect of aperture size and positions on heat

transfer rate at all boundary wall conditions and inclination of 90°. Finally effect of inclination angle on heat transfer rate will be presented.

Fig. 9 shows variation of $\overline{Nu}$ with Ra for different wall boundary conditions with the case of centrally located aperture of (AP = AR = 0.5) at inclinations of 90°. It is seen that the average Nusselt number increases rapidly with increasing Ra up to 10^4 thereafter the rate of increase in $\overline{Nu}$ decreases. At low Ra, boundary conditions have a minimal affect in $\overline{Nu}$ where conduction is the major mechanism for heat transfer out of the cavity regardless of the boundary wall condition. However, increasing Ra amplifies the boundary wall condition affect in increasing the Nusselt number. As expected it is observed that the heat transfer is higher for wall boundary condition case (D), i.e. when three walls from the cavity are heated.

Similar results are presented for the case of centrally located aperture of $AR = h/H$ = 0.75 in fig. 10. It is seen that with respect to the results in fig. 9, increased heat transfer at all boundary wall conditions due to larger aperture with less resistance to flow, which we have observed earlier with figs. 4 and 3-c. Again the highest Nusselt number is at boundary wall condition case (D) and the lowest in the case (B) for Ra up to 6×10^4 thereafter for the case case (C). The results with aperture of 0.25 centrally located not presented, show a similar trend for Nu of the case with 0.5 aperture size fig. 8 except the $\overline{Nu}$ is reduced due to relatively smaller aperture.

Fig. 11 shows variation of $\overline{Nu}$ with Ra at different aperture positions with the wall boundary condition case (A), AR = 0.5, and α = 90°. It is seen that the center aperture positions have a higher values of $\overline{Nu}$ than the other positions. Following the observations in figs. 5 and 3-c, at higher values of Ra (Ra > 8×10^4), the lower aperture positions have a values of $\overline{Nu}$ higher than these of center aperture positions.

Fig. 12 shows variation of average Nusselt number with Rayleigh number for wall boundary condition case (A) at various inclinations for the case of centerally located aperture

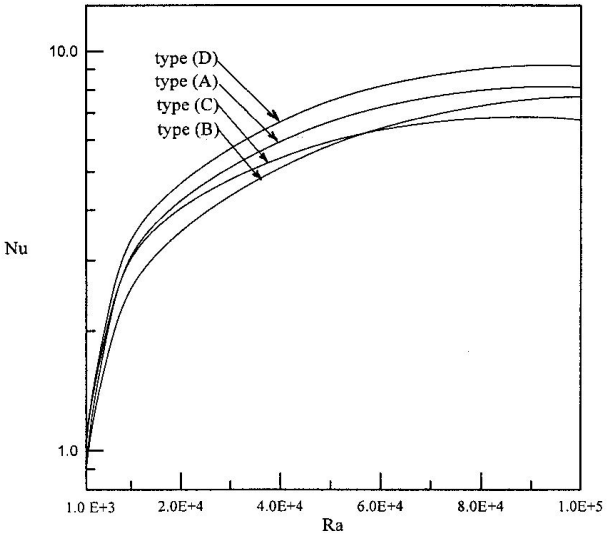

Fig. 9. Variation of Nu with Ra at different boundary wall conditions for the case of centrally located aperture (AP = 0.5, AR = 0.5) and inclination of 90°.

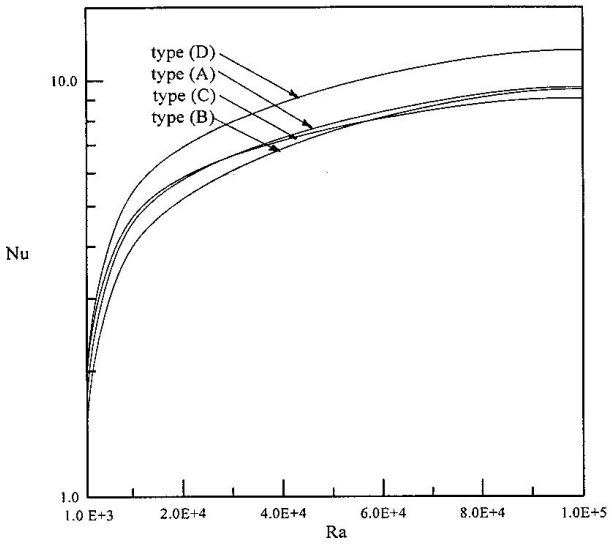

Fig. 10. Variation of Nu with Ra at different boundary wall conditions for the case of centrally located aperture (AP = 0.5, AR = 0.75) and inclination of 90°.

(AP = AR = 0.5). We see that at low inclination angle ($\alpha \le 60°$), the average Nusselt number increasing rapidly with increasing Ra up to 10^4 thereafter tapers off. At high inclination angle ($\alpha > 60°$), the average Nusselt number increases rapidly with increasing Ra. $\overline{Nu}$ is generally lower when the cavity aperture facing up and highest when horizontal i.e. α = 90°. This due to, at α = 90°, the flow that separates

at the lower edge of the opening reattaches on the base of the cavity and a single strong convection cell are formed in the cavity, as observations in fig. 7.

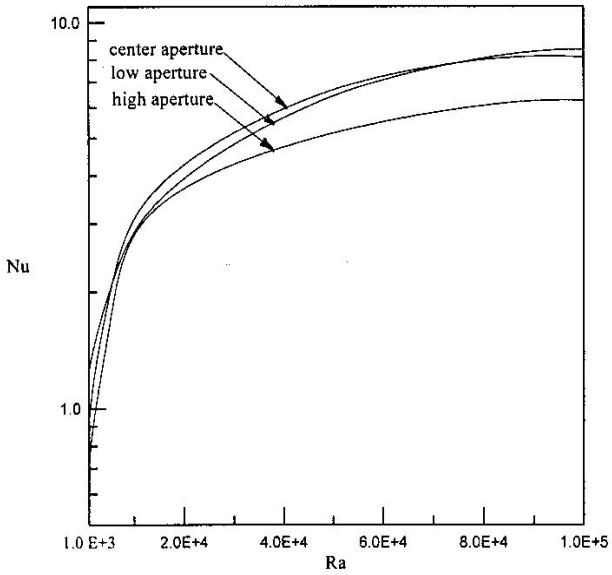

Fig. 11. Variation of *Nu* with Ra at different aperture position for the case of boundary wall condition type (A), AR = 0.5, and inclination of 90°.

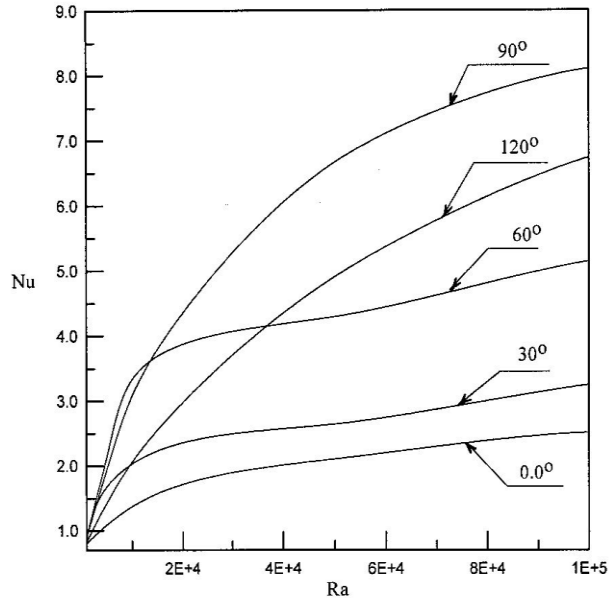

Fig. 12. Variation of Nu with Ra for boundary wall condition type (A) at various inclinations for the case of centerally located aperture (*AP* = *d*/*H* = 0.5, *AR* = *h*/*H* = 0.5).

5. Conclusions

Steady-state heat transfer by natural convection in partially open inclined square cavities with different wall boundary conditions has been numerically studied. Four cases of boundary wall conditions were studied: (a) case (A), the wall inside the cavity facing the partial opening and the lower wall are isothermal and the remaining walls are adiabatic, (b) case (B), the wall inside the cavity facing the partial opening and the upper wall are isothermal and the remaining walls are adiabatic, (c) case (C), the upper and lower walls are isothermal and the remaining walls are adiabatic, (d) case (D), the wall inside the cavity facing the partial opening, the lower and the upper walls are isothermal and the remaining walls are adiabatic. Dimensionless aperture size ranging from 0.25 to 0.75, with different positions: high, center and low. The tilt angles ranging from 0° (the opening facing upward) to 120° (the opening facing 30° downward) and the Rayleigh numbers between 10^3 to 10^5. It is found that tilt angle, wall boundary conditions, aperture size and position are all factors that strongly affect the convective heat transfer coefficient between the cavity and the ambient air. At low Ra, boundary conditions have a minimal affect in $\overline{Nu}$. However, increasing *Ra* amplifies the wall boundary condition affect in increasing the $\overline{Nu}$ Nusselt number. The heat transfer rate is higher for boundary wall condition case (D) compared to the other types. As aperture size increases the heat transfer increases for all boundary wall conditions due to larger aperture with less resistance to flow. The average Nusselt number ($\overline{Nu}$) is generally lower at low inclination angles ($\alpha \leq 30°$), and highest when the cavity horizontal ($\alpha = 90°$). Depending on the application, which may require maximizing or minimizing of heat transfer through the aperture, the wall boundary conditions, aperture size, its position and inclination angle should be chosen as design parameters.

Nomenclature

A is the enclosure aspect ratio, *H*/*L*,

AP is the dimensionless aperture position, d/H,
AR is the dimensionless aperture size, h/H,
c_p is the heat capacity, J/kg K,
g is the acceleration due to gravity, m/s^2,
H is the cavity height, m,
k is the thermal conductivity, W/m K,
L is the cavity width, m,
Nu is the Nusselt number, eq. (6),
p is the pressure, Pa,
P is the dimensionless pressure, $(p- p_\infty) L^2/ \rho\alpha^2$,
Pr is the Prandtl number, ν/α,
Ra is the Rayleigh number, $g\beta\Delta TL^3/(\nu\alpha)$,
t is the time, s,
ΔT is the temperature difference, $T - T_\infty$,
U,V is the dimensionless fluid velocities, uL/α, vL/α,
X,Y is the dimensionless Cartesian coordinates, x/L, y/L, and
x, y is the Cartesian coordinates.

Greek symbols

α is the thermal diffusivity, m^2/s,
β is the volumetric coefficient of thermal expansion, 1/K,
ν is the kinematic viscosity, m^2/s,
ρ is the fluid density, kg/m^3,
θ is the dimensionless temperature, $(T - T_\infty)/(T_H - T_\infty)$,
α is the inclination angle of cavity, o, and
τ is the dimensionless time, $\alpha t/L^2$.

Superscripts

$\bar{}$ is the average.

Subscripts

a is the air,
f is the fluid,
H is the hot,
loc is the local,
in is the into cavity,
ou is the out of cavity, and
∞ is the ambient value.

References

[1] V. Sernas and I. Kyriakides "Natural Convection in an Open Cavity", Proc. Seventh Int. Heat Transfer Conf. Munich, Vol. 2, pp. 275-280 (1982).

[2] C. F. Hess and R. H. Henze "Experimental Investigation of Natural Convection Losses From Open cavities", J. Heat Transfer, Vol. 106, pp. 333-338 (1984).

[3] Y.L. Chan and C.L. Tien "Laminar Natural Convection in Shallow Open Cavities", J. Heat Transfer, Vol. 108, pp. 305-309 (1986).

[4] R. A. Showole and J. D. Tarasuk "Experimental and Numerical Studies of Natural Convection with Flow Separation in Upward-Facing Inclined Open Cavities", Trans. ASME, J. Heat Transfer, vol. 115, pp. 592-605, (1993).

[5] W. Chakroun, M. M. Elsaey, and S.F. Al-Fahed "Experimental Measurements of Heat Transfer Coefficient in a Partially/Fully Opened Tilted Cavity", J. solar Eng., Vol. 119, pp. 298-303 (1997).

[6] M.M. Elsayed, and W. Chakroun, "Effect of Aperture Geometry on Heat Transfer in Tilted Partially Open Cavities", J. Heat Transfer, Vol. 121, pp. 819-827 (1999).

[7] F. Penot "Numerical Calculation of Two-Dimensional Natural Convection in Isothermal Open Cavities", Numerical Heat Transfer, Vol. 5, pp. 421-437 (1982).

[8] Y.L. Chan, and C.L. Tien "A Numerical Study of Two-Dimensional Natural Convection in Square Open Cavities", Numerical Heat Transfer, Vol. 8, pp. 65-80 (1985).

[9] M.M. Elsayed, N.M. Al-Najem, M.M. El-Refaee, and A. A Noor, "Numerical Study of Natural Convection in Fully Open Tilted Cavities", Heat Transfer Engineering, Vol. 20 (3), pp. 73-85 (1999).

[10] Y.L. Chan and C.L Tien "A Numerical Study of Two-Dimensional Laminar Natural Convection in shallow open cavities", Int. Heat Mass Transfer, Vol. 28, pp. 603-612 (1985).

[11] Y.L. Chan and C.L. Tien "Laminar Natural Convection in Shallow Open Cavities", Trans. ASME, J. Heat Transfer, Vol. 108, pp. 305-309 (1986).
[12] O. Polat, and E. Bilgen "Laminar Natural Convection in Inclined Open Shallow Cavities", Int. J. Thermal Sci. Vol. 41, pp. 360-368 (2002).
[13] G. Jilani, S. Jayarai, and K. Khadar "Numerical Analysis of Free Convective Flows in Partially open enclosure", Int. J. Heat Mass Transfer, Vol. 38 (3), pp. 261-270 (2002).
[14] E. Bilgen and H. Oztop "Natural Convection Heat Transfer in Partially Open Inclined Square cavities", Int. J. Heat Mass Transfer, Vol. 48 (8), pp. 1462-1469 (2005).
[15] Fluent 6.1.18 User's Guide, Volumes 1-5, Fluent Inc. (2002).

Received July 19, 2005
Accepted January 30, 2006